

On the High Order Approximation of the Centre Manifold for ODEs

Ariadna Farrés and Àngel Jorba

Departament de Matemàtica Aplicada i Anàlisi

Universitat de Barcelona

Gran Via 585, 08007 Barcelona, Spain

E-mails: ari@maia.ub.es, angel@maia.ub.es

1st September 2009

Abstract

Many times in dynamical systems one wants to understand the bounded motion around an equilibrium point. From a numerical point of view, we can take arbitrary initial conditions close to the equilibrium points, integrate the trajectories and plot them to have a rough idea of motion. If the dimension of the phase space is high, we can take suitable Poincaré sections and/or projections to visualise the dynamics. Of course, if the linear behaviour around the equilibrium point has an unstable direction, this procedure is useless as the trajectories will escape quickly. We need to get rid, in some way, of the instability of the system.

Here we focus on equilibrium points whose linear dynamics is a cross product of one hyperbolic directions and several elliptic ones. We will compute a high order approximation of the centre manifold around the equilibrium point and use it to describe the behaviour of the system in an extended neighbourhood of this point. Our approach is based on the graph transform method. To derive an efficient algorithm we use recurrent expressions for the expansion of the non - linear terms on the equations of motion.

Although this method does not require the system to be Hamiltonian, we have taken a Hamiltonian system as an example. We have compared its efficiency with a more classical approach for this type of systems, the Lie series method. It turns out that in this example the graph transform method is more efficient than the Lie series method. Finally, we have used this high order approximation of the centre manifold to describe the bounded motion of the system around and unstable equilibrium point.

Contents

| | | |
|----------|---|-----------|
| 1 | Introduction | 2 |
| 2 | Reduction to the Centre Manifold | 4 |
| 2.1 | Graph Transform | 5 |
| 2.1.1 | Scheme of the computation | 6 |
| 2.1.2 | Efficiency considerations | 8 |
| 2.2 | The Lie Series Method | 12 |
| 3 | The RTBP for a Solar Sails | 14 |
| 3.1 | Settings | 17 |
| 3.2 | Results | 19 |
| 3.2.1 | For the Graph Transform Method | 19 |
| 3.2.2 | For the Lies Series Method | 20 |
| 3.3 | Tests and Comparisons | 21 |
| 3.4 | Dynamics on the Centre Manifold | 25 |
| 4 | Conclusions | 27 |
| | REFERENCES | 28 |

1 Introduction

Our aim is to understand the dynamics in an extended neighbourhood of an unstable equilibrium point. We focus on those points whose linear dynamics is the cross product of a saddle and several complex directions with zero real part. We mainly want to describe the bounded motion around them. Due to the instability produced by the saddle, taking arbitrary initial conditions and integrating them numerically to produce plots of the orbits, is not a good option as the trajectories will escape quickly. To get rid of the instability produced by the saddle, we propose to perform the so - called reduction to the centre manifold.

We call centre manifold to an invariant manifold that is tangent to linear subspace generated by the different pairs of complex eigenvectors. We know that this invariant manifold might not be unique, although the Taylor expansion of the graph of this invariant manifold is [1, 14, 17]. The reduction to the centre manifold process consists in finding a high order approximation of this invariant manifold. The main idea is to uncouple the saddle direction from the other directions up to high order. Then, neglecting the reminder we have a high order approximation of the flow on an invariant manifold that does not contain the saddle.

In this way we can do numerical integrations and study the motion around the equilibrium point on the centre manifold.

If the system is Hamiltonian we can compute this manifold using a partial normal form scheme of the Hamiltonian [7]. Nevertheless, we are interested in a more general procedure, that does not take into account the Hamiltonian structure of the system. To deal with systems that are not Hamiltonian we propose the graph transform method. Here the idea is to compute, formally, the power expansion of the graph of the centre manifold around the equilibrium point [1, 15]. In Section 2 we describe the main ideas of these two methods.

As we will see, to apply the graph transform method we need to compose multivariate power series expansions, which can have a high computational cost. We will use recurrent expressions for the series expansion to derive an efficient algorithm. In section 2.1.2 we will show how this can be done.

We have applied this method to describe the dynamics of a solar sail close to equilibria in the Earth - Sun system. A solar sail is a proposed form of spacecraft propulsion, that takes advantage of the impact of the photons emitted by the Sun on large membrane mirrors to impulse the spacecraft. In the past years, the space industry has been testing the technology and studying possible near term mission applications for a solar sail. Although the acceleration due to the sail is very small compared to the acceleration that an engine can produce, it is continuous and unlimited. Hence, it opens a new range of possible mission applications that cannot be achieved by a regular spacecraft, for instance, remaining around a fixed point above of the ecliptic plane [3, 10, 11].

To model the dynamics of a solar sail we have considered the Circular Restricted Three Body Problem, taking the Earth and Sun as primaries, and added the effect of the solar radiation pressure (RTBPS). As we will see in Section 3 if the sail is oriented perpendicular to the Sun - line the system is Hamiltonian and has three equilibrium points of the type centre \times centre \times saddle. Moreover, there are other sail orientations where the system is no longer Hamiltonian, but it still has centre \times centre \times saddle equilibrium points. Hence, we need a procedure that allows us to study these other cases. In [2] we have used the techniques presented here to understand the dynamics around different equilibrium points when the system is not Hamiltonian.

We have consider the particular case of a solar sail oriented perpendicular to the Sun - line to compare the two different methods. We have taken the public domain software in [6] that performs the reduction to the centre manifold for the RTBP around $L_{1,2,3}$ [7, 8] and adapted it to our model. This software performs a partial normal form scheme on the Hamiltonian of the system using the Lie series method. We use this software to compare the two algorithms.

Surprisingly as it might seem, a suitable implementation of the graph transform method is more efficient than the Lie series method, in terms of computational time. Plus, it is a more general procedure that can be applied to any set of equations, Hamiltonian or non-

Hamiltonian. In Section 3.3 we discuss the efficiency of both methods.

Finally, we have applied the reduction to the centre manifold around two unstable equilibrium points of the RTBPS to describe the bounded motion in an extended neighbourhood of these points. In Section 3.4 we will show the existence of families of periodic and quasi-periodic orbits around them.

2 Reduction to the Centre Manifold

From now on we focus on a fixed point whose linear dynamics is the cross product of hyperbolic and elliptic directions. Our aim is to describe the dynamics on an extended neighbourhood of this point. In particular we are interested in those trajectories that remain close to the equilibrium point.

Usually, to have a first guess of the dynamics, we take a certain Poincaré section, iterate the Poincaré map for several initial conditions and plot suitable projections of the trajectory. If the system is Hamiltonian, we can do the same, taking initial conditions for a fixed energy level. In this way we reduce the phase space dimension by 2 and we can get an idea of the evolution of the system w.r.t the energy level.

It is a known fact that, close to an unstable equilibrium point, if we take arbitrary initial conditions and just integrate them numerically, the solution will escape from a vicinity of the equilibrium point with probability one. For this reason, we propose to do the reduction to the centre manifold around the equilibrium point and get rid of the hyperbolic character of the system.

The main idea is to expand the equations of motion around the equilibrium point and uncouple up to high order the hyperbolic directions from the elliptic ones. Then, neglecting the reminder we have a high order approximation of the centre manifold. We will use this approximation for numerical integrations and have a complete understanding of the bounded motion.

If we consider a Hamiltonian system, one can take advantage of its structure to compute the reduction to the centre manifold. We can expand the Hamiltonian around the equilibrium point and perform canonical transformations on the Hamiltonian to uncouple the two behaviours. This procedure is similar to the computation of the normal form, but here we kill less monomials. In [7, 8], this procedure was used to describe the motion around the collinear equilibrium points of the classical RTBP.

Nevertheless, we are interested in a more general scheme for the problem, without taking into account the Hamiltonian structure of the system. Then, we propose to compute, formally, the power series of the graph of the centre manifold at the equilibrium point [1]. This is known as the graph transform method and is a general procedure that can be used

for a general set of equations [15]. In Section 2.1 we give the details for the computation of the centre manifold using the graph transform method.

In this method one deals with the composition of power series, which can have a high cost in terms of computational time. We will use recurrent expressions to expand the non-linear terms, and use them to compose the power series in an efficient way. In Section 2.2 we recall the main ideas for the reduction to the centre manifold using this approach. Further on, in Section 3.3, we will compare the efficiency of this algorithm with the Lie series method for Hamiltonian systems.

For the sake of simplicity, from now on, we will always consider that we have a fixed point of the type centre \times centre \times saddle. However, the same techniques can be extended in an easy way for a more general case when the system has several “centres” and “saddles” [15].

As the general purpose algebraic manipulators are not efficient enough to deal with big expansions, we have written our own software from scratch, using ANSI C language. The algebraic manipulator that we have used is explained with full detail in [7]. These programs are built in different layers. In the bottom layer we have the routines corresponding to handle polynomials. Built on top are the routines using the algorithms for the actual reduction to the centre manifold that we will explain in the following lines.

In what follows, we will use the following notation. If $z = (z_1, \dots, z_\ell)$ is a vector of complex numbers and $k = (k_1, \dots, k_\ell)$ a vector of natural numbers, we denote $z^k = z_1^{k_1} \dots z_\ell^{k_\ell}$ (here, $0^0 = 1$). Moreover, we define $|k| = k_1 + \dots + k_\ell$.

2.1 Graph Transform

Let $\dot{z} = F(z)$, with $z \in \mathbb{R}^6$ and F smooth enough, be an ordinary differential equation with a fixed point of the type centre \times centre \times saddle. Without loss of generality we can assume that the fixed point is at the origin. It is well known that with an appropriate linear transformation, the equations of motion can be written as:

$$\begin{aligned}\dot{x} &= Ax + f(x, y), \\ \dot{y} &= By + g(x, y),\end{aligned}\tag{1}$$

where $x \in \mathbb{R}^4$, $y \in \mathbb{R}^2$, the eigenvalues of the matrix A have zero real part and the eigenvalues of the matrix B are real. The functions f and g are sufficiently smooth and satisfy,

$$f(0, 0) = 0, \quad Df(0, 0) = 0, \quad g(0, 0) = 0, \quad Dg(0, 0) = 0.$$

Note that $y = 0$ is the linear approximation to the centre manifold. We want to find $y = v(x)$ with $v(0) = 0$ and $Dv(0) = 0$, the local expression of the centre manifold. If we substitute

this on equations (1), we have that $v(x)$ must satisfy:

$$Bv(x) + g(x, v(x)) = Dv(x)[Ax + f(x, v(x))], \quad (2)$$

and the flow restricted to the manifold is given by,

$$\dot{x} = Ax + f(x, v(x)). \quad (3)$$

For further details see for instance [1]. Although the centre manifold might not be unique, its Taylor expansion at the equilibrium point is.

We want to find the Taylor expansion of the graph of the centre manifold at the equilibrium point, $v(x)$, truncated at high order. We call this high order approximation $\widehat{v}(x)$. Then we can take, $\dot{x} = Ax + f(x, \widehat{v}(x))$, to have a high order approximation of the motion on the centre manifold.

2.1.1 Scheme of the computation

Let us assume that we have already made a linear change of variables and set the equations as in (1) and let $\pm\lambda$, $\pm i\omega_1$ and $\pm i\omega_2$ be the eigenvalues of $D_z F$. We want to find $y = v(x)$ that satisfies equation (2).

We take $v(x) = \sum_{|k|\geq 2} v_k x^k$, with $v_k \in \mathbb{R}^2$, the formal power expansion of $v(x)$ around the origin. We are interested in knowing the values $v_k = (v_k^1, v_k^2)$ up to high order to have a good approximation of the centre manifold near the point. For instance, if we have $\widehat{v}(x) = \sum_{|k|=2}^N v_k x^k$ that satisfies equation (2) up to order N , then $\widehat{v}(x)$ approximates the graph of the centre manifold up to the same order, i.e. $\|v(x) - \widehat{v}(x)\| = O(\|x\|^N)$.

Notice that equation (2) can be rewritten as,

$$Dv(x)Ax - Bv(x) = g(x, v(x)) - Dv(x)f(x, v(x)), \quad (4)$$

where, the left - hand side of this equation is a linear operator w.r.t $v(x)$ and the right - hand side a non linear one.

If we assume A and B to be in diagonal form, $A = \text{diag}(i\omega_1, -i\omega_1, i\omega_2, -i\omega_2)$ and $B = \text{diag}(\lambda, -\lambda)$, then the left - hand side of equation (4) also takes a diagonal form,

$$Dv(x)Ax - Bv(x) = \begin{pmatrix} \sum_{|k|\geq 2} (i\omega_1 k_1 - i\omega_1 k_2 + i\omega_2 k_3 - i\omega_2 k_4 - \lambda) v_{1,k} x^k \\ \sum_{|k|\geq 2} (i\omega_1 k_1 - i\omega_1 k_2 + i\omega_2 k_3 - i\omega_2 k_4 + \lambda) v_{2,k} x^k \end{pmatrix}. \quad (5)$$

Let $h(x) = g(x, v(x)) - Dv(x)f(x, v(x))$ be the right hand side of equation (4). We take its expansion $h(x) = \sum_{|k| \geq 2} h_k x^k$ around the origin ($h_k = (h_k^1, h_k^2)$), where the coefficients h_k depend on the coefficients v_k in a known way. As we will see in Lemma 2.2, the coefficients h_k for $|k| = n$ depend on v_k with $|k| < n$. This allows us to find the v_k in an iterative way.

Let us see how to arrange the terms v_k of degree 2. We take the power expansion of $f(x, y)$ and $g(x, y)$ around the origin,

$$f(x, y) = \sum_{|k_1|+|k_2| \geq 2} f_{k_1, k_2} x^{k_1} y^{k_2}, \quad g(x, y) = \sum_{|k_1|+|k_2| \geq 2} g_{k_1, k_2} x^{k_1} y^{k_2},$$

where the $f_{k_1, k_2} \in \mathbb{R}^4$ and $g_{k_1, k_2} \in \mathbb{R}^2$ are known. Now we take $v(x)$ up to degree 2,

$$v(x) = \sum_{|k|=2} v_k x^k,$$

and we substitute this on equation (4) and equalise the terms of degree 2. As $Dv(x)$ and $f(x, v(x))$ start with monomials of degree 1 and 2 respectively, their product $Dv(x)f(x, v(x))$ starts with monomials of degree 3. Hence, for $|k| = 2$ we have that $h_k = g_{k,0}$. Then the degree 2 terms on equation (4) satisfy,

$$\sum_{|k|=2} (i\omega_1 k_1 - i\omega_1 k_2 + i\omega_2 k_3 - i\omega_2 k_4 \mp \lambda) v_k x^k = \sum_{|k|=2} g_{k,0} x^k,$$

as $\lambda \neq 0$, we can find all the coefficients v_k , by equalising each of the monomials with $|k| = 2$. Having:

$$v_k^1 = \frac{g_{k,0}^1}{i\omega_1 k_1 - i\omega_1 k_2 + i\omega_2 k_3 - i\omega_2 k_4 - \lambda}, \quad v_k^2 = \frac{g_{k,0}^2}{i\omega_1 k_1 - i\omega_1 k_2 + i\omega_2 k_3 - i\omega_2 k_4 + \lambda}.$$

To arrange the higher order terms we proceed in the same way. For a given degree $\ell > 2$, we:

1. Take $v(x)$ up to degree ℓ , $\left(\sum_{|k| \geq 2}^{\ell} v_k x^k\right)$.
2. Substitute it on equation (4) and find the values of the coefficients h_k for $|k| = \ell$. Notice that the coefficients h_k depend on the coefficients f_{k_1, k_2} , g_{k_1, k_2} with $|k_1| + |k_2| \leq \ell$ and v_k with $|k| < \ell$.
3. Finally, we equalise the degree ℓ terms on equation (4), and solve the diagonal system to find the coefficients v_k for $|k| = \ell$.

This process is carried out for $\ell = 3, 4, \dots$, up to a sufficiently high order N . In the end we have the expansion $\widehat{v}(x)$ up to degree N , a high order approximation of the centre manifold

($\|v(x) - \widehat{v}(x)\| = O(x^N)$):

$$\widehat{v}(x) = \sum_{|k| \geq 2}^N v_k x^k. \quad (6)$$

Once we have $\widehat{v}(x)$, we are ready to explore the phase space. We will use $\dot{x} = Ax + f(x, \widehat{v}(x))$, to integrate the flow, as it gives a high order approximation of the motion on the centre manifold. Notice that during the reduction process we also compute $f(x, \widehat{v}(x))$, so we can store it while we are computing it.

We must recall, that we can find the coefficients v_k in an iterative way solving a diagonal linear system degree by degree, because the coefficients h_k for $|k| = \ell$, depend on the coefficient of v_k with $|k| < \ell$ (Lemma 2.2) and the matrices A and B are in diagonal form.

Remark 1 *The linear system can be solved if and only if*

$$i\omega_1 k_1 - i\omega_1 k_2 + i\omega_2 k_3 - i\omega_2 k_4 \mp \lambda \neq 0,$$

which is always true as $\lambda \in \mathbb{R} \setminus \{0\}$ and $i\omega_1, i\omega_2$ are pure imaginary numbers.

Remark 2 *It is not necessary to have A and B in their diagonal form, but then the linear part of equation (4) will not take a diagonal form. Then, as we increase the degree, the dimension of the linear system we have to solve increases and so does the computational cost and error propagation to solve it.*

Remark 3 *To have A in its diagonal form, we need to take an initial complex change of variables. Hence, we need to apply the inverse of this change to the final representation $\widehat{v}(x)$ in the real set of coordinates.*

Remark 4 *To have an efficient algorithm, we need to have an efficient way to compute the coefficients h_k . These coefficients come from the expansion around the origin of*

$$h(x) = g(x, v(x)) - Dv(x)f(x, v(x)).$$

Expanding $g(x, y)$ and $f(x, y)$ and then composing with $v(x)$ is not an option, as the composition of multivariate series is very expensive in terms of computational time. Instead, we will use recurrent expressions for the expansion of these functions to obtain a more efficient algorithm. In the next section we give further details in this direction.

2.1.2 Efficiency considerations

Let us see how to use recurrent expressions for the expansion of functions $f(x, y)$ and $g(x, y)$ around the origin to derive an efficient algorithm to compute the coefficients h_k of the Taylor expansion of $h(x) = g(x, v(x)) + Dv(x)f(x, v(x))$.

Let us assume that we have:

$$f(x, y) = \sum_{n \geq 2} F_n(x, y), \quad g(x, y) = \sum_{n \geq 2} G_n(x, y),$$

where $F_n(x, y)$ and $G_n(x, y)$ are homogeneous polynomials of degree n that are found in a recurrent way. This means that there exist two functions $R_1(\zeta_1, \dots, \zeta_j)$ and $R_2(\zeta_1, \dots, \zeta_j)$ such that,

$$F_{n+1} = R_1(F_n, \dots, F_{n-j}), \quad G_{n+1} = R_2(G_n, \dots, G_{n-j}), \quad (7)$$

where the F_2, \dots, F_j and G_2, \dots, G_j are known, and R_1 and R_2 only contain simple arithmetic operations between polynomials ($+ / - / \times$).

Let us start with a couple of lemmas on these recurrences and polynomial expressions.

Lemma 2.1 *Let $f : \mathcal{U}_1 = \overset{\circ}{\mathcal{U}}_1 \subset \mathbb{R}^4 \times \mathbb{R}^2 \mapsto \mathbb{R}^m$, with $0 \in \mathcal{U}_1$, $m > 0$, and $v : \mathcal{U}_2 = \overset{\circ}{\mathcal{U}}_2 \subset \mathbb{R}^4 \mapsto \mathbb{R}^2$, with $0 \in \mathcal{U}_2$ be two \mathcal{C}^∞ functions, such that,*

$$f(x, y) = \sum_{n \geq 2} F_n(x, y), \quad v(x) = \sum_{n \geq 2} V_n(x), \quad \text{on a neighbourhood of } 0,$$

where $F_n(x, y)$ and $V_n(x)$ are homogeneous polynomials of degree n . Then,

- (a) $F_n(x, v(x))$ is a polynomial that starts at degree n .
- (b) the coefficients of $F_n(x, v(x))$ that depend on the coefficients of $v(x)$ are of degree $r \geq n + 1$.
- (c) the coefficients of $F_n(x, v(x))$ of degree r depend on the coefficients of $v(x)$ of degree $k < r$.

It immediately follows that the coefficients of $f(x, v(x))$ of degree r depend on the coefficients of $v(x)$ of degree $k < r$.

Proof: Let us start by taking a homogeneous polynomial of $f(x, y)$ of degree n . It is clear that $F_n(x, y)$ can be expressed as,

$$F_n(x, y) = \sum_{|k_1|+|k_2|=n} f_{k_1, k_2} x^{k_1} y^{k_2}, \quad k_1 \in (\mathbb{N} \cup \{0\})^4, \quad k_2 \in (\mathbb{N} \cup \{0\})^2$$

where f_{k_1, k_2} are the coefficients of the homogeneous polynomial. Then,

$$F_n(x, v(x)) = \sum_{|k_1|+|k_2|=n} f_{k_1, k_2} x^{k_1} \left(\sum_{i \geq 2} V_i(x) \right)^{k_2}.$$

Notice that $(\sum_{i \geq 2} V_i(x))^{k_2}$ is a polynomial that starts at degree $2|k_2|$. Hence, the coefficients of $F_n(x, v(x))$ have at least degrees $|k_1| + 2|k_2|$. Assuming that $|k_1| + |k_2| = n$, the minimum takes place for $|k_2| = 0$, hence $F_n(x, v(x))$ is a homogeneous polynomial that starts at degree n .

Let us now take a look on which coefficients of $F_n(x, v(x))$ depend on the coefficients of $v(x)$. It is clear that the monomials that depend on the coefficient of $v(x)$ come from the terms $f_{k_1, k_2} x^{k_1} (\sum_{i \geq 2} V_i(x))^{k_2}$ with $|k_2| \neq 0$. As we have already seen, these terms have degree at least $|k_1| + 2|k_2|$. As $|k_1| + |k_2| = n$, then $|k_1| + 2|k_2| = n + |k_2|$. Hence, the terms $f_{k_1, k_2} x^{k_1} (\sum_{i \geq 2} V_i(x))^{k_2}$ that depend on the coefficients of $v(x)$ are of degree at least $n + 1$.

Let $\tilde{f}_k x^k$ be a monomial of $F_n(x, v(x))$ of degree $|k| = r \geq n + 1$. Hence, as already seen, it depends on the coefficients of $v(x)$. We want to see that \tilde{f}_k depends on coefficient of $v(x)$ of degree less than r .

Let us take a coefficient v_k of degree $|k| = s$ on $v(x)$, and see to what degree it corresponds after the composition. Notice that if we take a coefficient of degree s on $(\sum_{i \geq 2} V_i(x))^{k_2}$, it ends up appearing in different monomials. As $1 \leq |k_2| \leq n$, we can say that the monomials of minimum degree in which it will appear are of degree s for $|k_2| = 1$ and $s + 1$ for $|k_2| > 1$.

We take $f_{k_1, k_2} x^{k_1} (\sum_{i \geq 2} V_i(x))^{k_2}$. Now the coefficients of $v(x)$ are being multiplied by x^{k_1} , hence the minimal degrees s for $|k_2| = 1$ and $s + 1$ for $|k_2| > 1$, are now, $s + |k_1|$ for $|k_2| = 1$ and $s + 1 + |k_1|$ for $|k_2| > 1$. Finally, as $|k_1| + |k_2| \geq 2$ we can assure that a coefficient of degree s on $v(x)$ will end up appearing on a coefficient of degree $s + 1$ on $F_n(x, v(x))$. Hence, if \tilde{f}_k is a coefficient of degree $|k| = r$ on $F_n(x, v(x))$, it can only depend on coefficients of $v(x)$ of degree at most $r - 1$.

□

Lemma 2.2 Let $h : \mathcal{U} = \overset{\circ}{\mathcal{U}} \subset \mathbb{R}^4 \mapsto \mathbb{R}^2$, with $0 \in \mathcal{U}$ be a C^∞ function defined as:

$$h(x) = g(x, v(x)) - Dv(x)f(x, v(x)),$$

where $f : \mathcal{U}_1 = \overset{\circ}{\mathcal{U}}_1 \subset \mathbb{R}^4 \times \mathbb{R}^2 \mapsto \mathbb{R}^4$, $g : \mathcal{U}_2 = \overset{\circ}{\mathcal{U}}_2 \subset \mathbb{R}^4 \times \mathbb{R}^2 \mapsto \mathbb{R}^2$, $v : \mathcal{U}_3 = \overset{\circ}{\mathcal{U}}_3 \subset \mathbb{R}^4 \mapsto \mathbb{R}^2$, with $0 \in \mathcal{U}_i$ for $i = 1, 2, 3$, $f, g, v \in C^\infty$ and that satisfy,

$$f(0, 0) = 0, \quad Df(0, 0) = 0; \quad g(0, 0) = 0, \quad Dg(0, 0) = 0; \quad v(0) = 0, \quad Dv(0) = 0.$$

Then, the coefficients of the Taylor expansion of $h(x)$, of degree n depend on the Taylor coefficients of $v(x)$ of degree $k < n$.

Proof: It is clear that the Taylor expansions of $f(x, y)$, $g(x, y)$ and $v(x)$ around the origin

can be written as:

$$g(x, y) = \sum_{n \geq 2} G_n(x, y), \quad f(x, y) = \sum_{n \geq 2} F_n(x, y), \quad v(x) = \sum_{n \geq 2} v_n(x),$$

where $G_n(x, y)$, $F_n(x, y)$ and $V_n(x)$ are homogeneous polynomials of degree n . From Lemma 2.1 we have that the coefficients of the Taylor expansion of $g(x, v(x))$ and $f(x, v(x))$ of degree n depend only on the coefficients of the Taylor expansion of $v(x)$ of degree $r < n$.

It is also clear that the coefficients on the Taylor expansion of $Dv(x)$ of degree n now depend on the coefficients of $v(x)$ of degree $n + 1$. To prove the lemma we just need to see that the coefficients of degree n of $Dv(x)f(x, v(x))$ depend only on the coefficients of $v(x)$ of degree $k < n$.

Notice that $f(x, v(x))$ starts at degree 2, then a monomial of degree s of $Dv(x)$, will contribute to the monomials of degree at least $s + 2$ on $Dv(x)f(x, v(x))$. Hence, the coefficients of degree n on $v(x)$, will appear only on the coefficients of degree at least $n + 1$ on $Dv(x)f(x, v(x))$.

□

Lemma 2.2 assures that the algorithm for the reduction to the centre manifold, explained above, can be applied in an iterative way.

Now, let us focus on the efficient computation of the coefficients of $h(x)$. We recall that

$$h(x) = g(x, v(x)) + Dv(x)f(x, v(x)). \quad (8)$$

We will use the recurrent expressions (7) for the coefficients of $g(x, y)$ and $f(x, y)$.

Let us assume that we know $v(x)$ up to degree r and we want to find the coefficients of degree $r + 1$. Hence, as mentioned in Section 2.1.1 we first need to find the coefficients of $h(x)$ of degree $r + 1$ and then solve the diagonal linear system (4). We start by finding the coefficients of $f(x, v(x))$ and $g(x, v(x))$ of degree $r + 1$. Once this is done, we can compute the coefficients of degree $r + 1$ of $h(x)$ using equation(8). Let us focus on $f(x, v(x))$, the same ideas apply for $g(x, v(x))$.

We recall that $f(x, y) = \sum_{n \geq 2} F_n(x, y)$, where the $F_n(x, y)$ are homogeneous polynomials of degree n . From lemma 2.1 we have that $F_n(x, v(x))$ is a polynomial that starts at degree n , hence, if we want the coefficients of $f(x, v(x))$ of degree $r + 1$, we just need to find, $F_2(x, v(x)), \dots, F_{r+1}(x, v(x))$. Here is where the recurrent expressions for F_j play an important role.

For the sake of simplicity, let us assume that $F_2(x, y)$ and $F_3(x, y)$ are known, and that

$$F_n(x, y) = R_1(F_{n-1}(x, y), F_{n-2}(x, y)), \quad \text{for } n > 3,$$

where R_1 are basic arithmetic operation between polynomials. We use this expression to find the polynomials, $F_2(x, v(x)), \dots, F_{r+1}(x, v(x))$ and then add them up to have $f(x, v(x))$ up to degree $r + 1$.

Once we have $f(x, v(x))$ and $g(x, v(x))$ up to degree $r + 1$, we easily compute $h(x)$ up to degree $r + 1$ using equation (8) and operating with the full polynomials.

This process will be repeated up to the desired final degree N . At each step we need to run this recurrent scheme up to the desired degree. For some particular recurrences one can take advantage of its properties to save computational time. Notice that for each degree r we are recomputing the terms of degree $s < r$ that we already have.

In Section 3.1 we will show how to expand the RTBPS equations in a recurrent way. We have used the Legendre polynomial recurrences to find such expressions. Although there are other ways of expanding the equations in a recurrent way, one can considered, for instance, automatic differentiation tools [9, 5].

2.2 The Lie Series Method

When the system is Hamiltonian, we can uncouple the hyperbolic from the elliptic behaviour by performing the changes of variables directly on the Hamiltonian (one equation) instead of doing it to the whole set of equations. Hence, we save computational effort. To do this, we need the changes of variables to be canonical to preserve the Hamiltonian structure of the system.

In [4, 7, 8] this procedure is applied to the RTBP around the collinear points $L_{1,2,3}$, and a public domain software for this purpose is available in [6]. In [13] we find a way to implement these algorithms using parallel computation. We have adapted the public domain software in [6] to our system of a Solar sail in the RTBP. We will use it to compare and contrast the results given by the graph transform method. Let us summarise the main ideas of this algorithm, for further details see [7].

Let H be a real analytic Hamiltonian of 3 degrees of freedom, that has an equilibrium point of the type centre \times centre \times saddle. Let $\pm\lambda, \pm i\omega_1$ and $\pm i\omega_2$ be the eigenvalues of the linearised system. Without loss of generality we can assume that the fixed point is at the origin. We start by expanding the Hamiltonian H around the origin, taking the complex coordinates for which the second degree terms take the diagonal form,

$$H(q, p) = H_2(q, p) + H_3(q, p) + H_4(q, p) + \dots, \quad (9)$$

where $H_j(q, p)$ are homogeneous polynomials of degree j in the variables (q, p) , where q

corresponds to the position and p to the momentum, and

$$H_2(q, p) = \lambda q_1 p_1 + i\omega_1 q_2 p_2 + i\omega_2 q_3 p_3. \quad (10)$$

Notice that the linear hyperbolic character is given by the couple (q_1, p_1) while the other variables define the centre behaviour. In order to decouple the hyperbolic direction from the elliptic one up to high order, we do not need to kill all the possible monomials, just the ones such that the exponent of p_1 is different from the one of q_1 . There are other killing criteria that can be considered, (see [4]), but this one allows us to end up having a first integral.

The changes of variables are implemented by means of the Lie series method. If $G(q, p)$ is a Hamiltonian system, the change of variables given by the time one flow corresponding to G is a canonical change of variables. The result of applying this change on H is:

$$\widehat{H} = H + \{H, G\} + \frac{1}{2!} \{\{H, G\}, G\} + \frac{1}{3!} \{\{\{H, G\}, G\}, G\} + \dots, \quad (11)$$

where G is usually called the generating function. These are the kind of canonical transformations that we deal with.

Now we can start the reduction to the centre manifold. The main idea is to perform a sequence of transformations like (11) in order to kill degree by degree the desired monomials of H . To see how this is done, let us give the ideas on how to arrange degree three.

Let us select as a generating function $G_3(q, p)$, a homogeneous polynomial of degree three. It is not difficult to see that if P and Q are two homogeneous polynomials of degree r and s respectively, then $\{P, Q\}$ is also a homogeneous polynomial of degree $r + s - 2$. Hence, the terms of \widehat{H} satisfy

$$\text{degree 2: } \widehat{H}_2 = H_2,$$

$$\text{degree 3: } \widehat{H}_3 = H_3 + \{H_2, G_3\},$$

$$\text{degree 4: } \widehat{H}_4 = H_4 + \{H_3, G_3\} + \frac{1}{2!} \{\{H_2, G_3\}, G_3\},$$

⋮

We just want to kill those monomials of degree three such that the exponents on q_1 and p_1 are different. We look for a G_3 such that, $\{H_2, G_3\} + H_3$ has these monomials equal to zero. For the monomials that we do not want to kill we take the coefficients $g_{k_q, k_p} = 0$. One can be checked that [7],

$$G_3(q, p) = \sum_{(k_p, k_q) \in S_3} \frac{-h_{k_q, k_p}}{\langle k_p - k_q, \eta \rangle} q^{k_q} p^{k_p},$$

where S_n , $n \geq 3$ is the set of indexes (k_p, k_q) such that $|k_p| + |k_q| = n$ and have the first component of k_p different from the first component of k_q .

With this change we end up having,

$$\widehat{H}(q, p) = H_2(q, p) + \widehat{H}_3(q, p) + \widehat{H}_4(q, p) + \dots,$$

where $\widehat{H}_3(q, p)$ has the prescribed form. We proceed in an iterative way, killing the monomials $q^{k_q} p^{k_p}$ with $(k_q, k_p) \in S_n$, for $n = 4, 5, \dots$. This process is carried up to sufficiently high order N . After all the transformations the Hamiltonian takes the form,

$$\widehat{H} = H^{(N)}(q_1 p_1, q_2, p_2, q_3, p_3) + R(q_1, p_1, q_2, p_2, q_3, p_3),$$

where $H^{(N)}$ is the part of the Hamiltonian that we have arranged and R denotes the reminder. If we neglect the reminder and take $q_1 p_1 = 0$, we are skipping the hyperbolic part of $H^{(N)}$. The resulting Hamiltonian is the Hamiltonian of the flow inside an approximation of the centre manifold. So near the origin the phase space of the original Hamiltonian must be the phase space of $H^{(N)}(0, q_2, p_2, q_3, p_3)$ times the hyperbolic direction.

It is important to notice the absence of small divisors in all the process. One can check that if $(k_p, k_q) \in S_n$, as $\lambda \in \mathbb{R} \setminus \{0\}$ then $|\langle k_q - k_p, \nu \rangle| \geq |\lambda|$. Hence, the divergence of this process is very mild. This makes the reminder to be small in a sufficiently large neighbourhood of the equilibrium point when this process is stopped for a certain N .

We recall that to have H_2 in a diagonal form we entered the complex phase space. So once we have finished the reduction process we need to apply the inverse of this change of variable to have the Hamiltonian $H^{(N)}$ in real coordinates. Notice that this is not necessary to do numerical integrations and understand the dynamics, but it is useful, as the operations with real arithmetic are faster than with complex arithmetic.

3 The RTBP for a Solar Sails

To describe the motion of a solar sail in the Earth - Sun system, we have taken the Restricted Three Body Problem for a Solar Sail (RTBPS). We have assumed that the Earth and Sun are point masses moving in a circular orbit around their common centre of mass, and the sail is a massless particle that is affected by the gravitational attraction of both bodies and the solar radiation pressure. The units of mass, distance and time are normalised so that the total mass of the system is 1, the Earth - Sun distance is 1 and the period of its orbit is 2π . We use a rotation reference system so that Earth and Sun are fixed on the x - axis, z is perpendicular to the ecliptic plane and y defines an orthogonal positive oriented reference system (Figure 1).

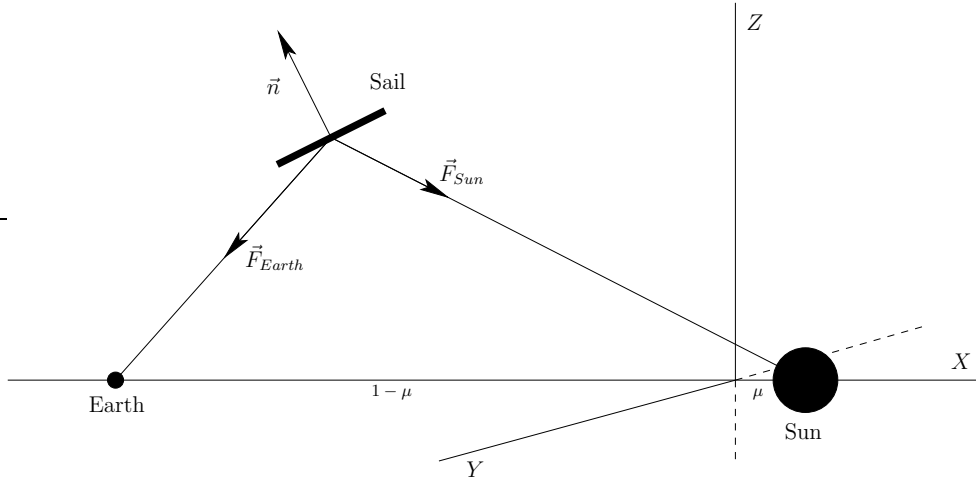


Figure 1: Schematic representation of model and forces acting in the RTBPS. Here \vec{F}_{Earth} and \vec{F}_{Sun} refer to the gravitational attraction due to the Earth and Sun respectively, and \vec{n} is the normal direction to the surface of the sail.

We will consider the solar sail to be flat and perfectly reflecting. This means that the force due to the solar radiation pressure is in the normal direction to the surface of the sail. In such case, the force due to the sail is given by,

$$\vec{F}_{sail} = \beta \frac{1 - \mu}{r_{PS}^2} \langle \vec{r}_s, \vec{n} \rangle^2 \vec{n},$$

where β represents the sail lightness number, \vec{r}_s is the Sun - line direction and \vec{n} is the normal direction to the surface of the sail (both vectors have norm 1). In this paper we consider the particular case of a sail oriented perpendicular to the Sun - line, where the system is Hamiltonian and with lots of similarities with the RTBP as we will see. We will use this example to compare the two different methods explained in the previous Section.

The equations of motion are,

$$\ddot{X} - 2\dot{Y} = \frac{\partial \Omega}{\partial X}, \quad \ddot{Y} + 2\dot{X} = \frac{\partial \Omega}{\partial Y}, \quad \ddot{Z} = \frac{\partial \Omega}{\partial Z}, \quad (12)$$

where,

$$\Omega(X, Y, Z) = \frac{1}{2} (X^2 + Y^2 + Z^2) + \frac{(1 - \mu)(1 - \beta)}{r_{PS}} + \frac{\mu}{r_{PE}}.$$

We can appreciate a resemblance with the RTBP, they only differ in a factor $(1 - \beta)$ on the potential force due to the Sun. Notice that setting the sail perpendicular to the Sun - line, is like reducing the Sun's gravitational attraction. This system also has a first integral,

$$J_C = \dot{X}^2 + \dot{Y}^2 + \dot{Z}^2 - 2\Omega(X, Y, Z).$$

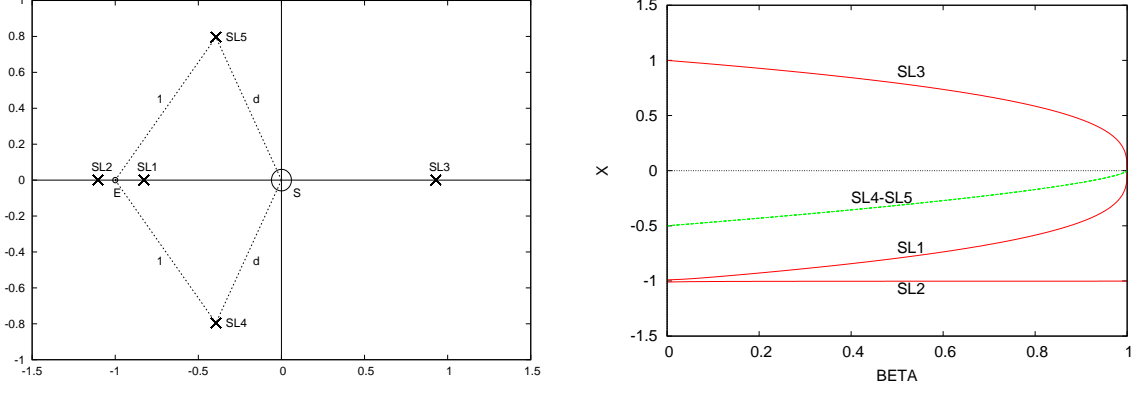


Figure 2: *Left: Schematic representation of the position of the equilibrium points SL_i for $i = 1, \dots, 5$ for a fixed β , where S stands for Sun, E for Earth and $d = (1 - \beta)^{1/3}$. Right: x component of the fixed points for $\beta \in [0, 1]$, we can see that they come closer to the Sun $\beta \rightarrow 1$.*

If we define the momenta $P_X = \dot{X} - Y$, $P_Y = \dot{Y} + X$ and $P_Z = \dot{Z}$, as in the classical RTBP, the equations can be written in a Hamiltonian form. The corresponding Hamilton equation is,

$$H = \frac{1}{2} (P_X^2 + P_Y^2 + P_Z^2) + YP_X - XP_Y - \frac{(1 - \mu)(1 - \beta)}{r_{PS}} - \frac{\mu}{r_{PE}}. \quad (13)$$

It can be seen that in synodical coordinates this model has five equilibrium points, named $SL_{1,\dots,5}$, that lie on the ecliptic plane. Three of them lie on the X - axis, they are called collinear points or $SL_{1,2,3}$ and are linearly unstable. The other two are the third vertex of an isosceles triangle with the two primaries on the other vertexes, they are called triangular points or $SL_{4,5}$ and are linearly stable. On the left - hand side of Figure 2, we show a schematic representation of the relative position of these points for a fixed β .

Following the same ideas as in [16] for the RTBP, we can find equivalent quintics to determine the position of the fixed points with respect to β , and a closed form for the position of $SL_{4,5}$. Let $\xi_{1,2}$ be the distance to the Earth and ξ_3 the distance to the Sun, then the three collinear points are,

$$SL_1 = (\mu - 1 + \xi_1, 0, 0), \quad SL_2 = (\mu - 1 - \xi_2, 0, 0), \quad SL_3 = (\mu + \xi_3, 0, 0),$$

where $\xi_{1,2,3}$ are the unique positive solution of the quintics.

$$\xi_1^5 - (3 - \mu)\xi_1^4 + (3 - 2\mu)\xi_1^3 - (\mu + \beta - \mu\beta)\xi_1^2 + 2\mu\xi_1 - \mu = 0,$$

$$\xi_2^5 + (3 - \mu)\xi_2^4 + (3 - 2\mu)\xi_2^3 - (\mu - \beta + \mu\beta)\xi_2^2 - 2\mu\xi_2 - \mu = 0,$$

$$\xi_3^5 + (2 + \mu)\xi_3^4 + (1 + 2\mu)\xi_3^3 - (1 - \mu)(1 - \beta)\xi_3^2 - 2(1 - \mu)(1 - \beta)\xi_3 - (1 - \mu)(1 - \beta) = 0.$$

The other two fixed points $SL_{4,5}$ are,

$$\left(\mu - \frac{(1-\beta)^{2/3}}{2}, \pm(1-\beta)^{1/3} \left(1 - \frac{(1-\beta)^{2/3}}{4} \right)^{1/2}, 0 \right),$$

where the upper sign is for SL_5 and the lower one for SL_4 . On the right - side of Figure 2, we show the variation of the x coordinate of the fixed point w.r.t. β . We can see that they all come closer to the Sun, where $SL_{1,3,4,5}$ collide with it for $\beta = 1$. Notice that taking $\beta = 1$ is like considering a sail that exerts a force on the spacecraft of the same magnitude as the Sun's gravitational attraction.

We want to understand the dynamics in an extended neighbourhood of the unstable equilibrium points $SL_{1,2}$, as they are the most relevant positions for possible mission applications. For instance, SL_1 lies between the Earth and the Sun and closer to the Sun than the classical L_1 , it is an ideal position to make observations of the Sun's geomagnetic storms. In this paper we have considered $\beta = 0.051689$, which corresponds to a sail loading of $30g/m^2$. This values are considered as realistic for a short term mission application, for instance the Geostorm Mission, see [10].

3.1 Settings

To start the reduction to the centre manifold process we need to express the linear part of the equations in a canonical way. Moreover, to have an efficient algorithm, we need a recurrent expressions for the non - linear terms. We use the Legendre Polynomials for this purpose, this recurrences are commonly used to expand the RTBP, see for instance [8, 7, 12].

We start by translating the origin of coordinates to one of the fixed points $SL_{1,2,3}$, using

$$X = \mp \xi_i x + \mu + a_i, \quad Y = \mp \xi_i y, \quad Z = \xi_i z, \quad (14)$$

where the upper sign corresponds to $SL_{1,2}$ and the lower to SL_3 , $a_1 = -1 + \xi_1$, $a_2 = -1 - \xi_2$ and $a_3 = \xi_3$. To have good numerical properties for the coefficients of the Taylor expansion, we scale the distance from the fixed point to the closest primary to one.

To find a recurrent expression for the expansion of the non - linear terms we use that:

$$\frac{1}{\sqrt{(x-A)^2 + (y-B)^2 + (z-C)^2}} = \frac{1}{D} \sum_{n=0}^{\infty} \left(\frac{\rho}{D} \right)^n P_n \left(\frac{Ax + By + Cz}{D} \right),$$

where $D^2 = A^2 + B^2 + C^2$, $\rho^2 = x^2 + y^2 + z^2$ and P_n is the Legendre polynomial of degree n . As it is done for the RTBP in [8, 7, 12], after some computations one obtains that the equations of motion around the equilibrium point in these new coordinates can be written

as,

$$\begin{aligned}
\ddot{x} - 2\dot{y} - (1 + 2c_2)x &= \sum_{n \geq 2} (n+1)c_{n+1}(\mu, \beta)T_n(x, y, z), \\
\ddot{y} + 2\dot{x} + (c_2 - 1)y &= y \sum_{n \geq 2} c_{n+1}(\mu, \beta)R_{n-1}(x, y, z), \\
\ddot{z} + c_2z &= z \sum_{n \geq 2} c_{n+1}(\mu, \beta)R_{n-1}(x, y, z),
\end{aligned} \tag{15}$$

where the left - hand side contains the linear terms and the right - hand side the nonlinear ones, $T_n(x, y, z)$ and $R_n(x, y, z)$ are homogeneous polynomial of degree n that satisfies the recurrences,

$$T_n = \frac{2n-1}{n}xT_{n-1} - \frac{n-1}{n}(x^2 + y^2 + z^2)T_{n-1}, \tag{16}$$

with $T_0 = 1$ and $T_1 = x$.

$$R_n(x, y, z) = \frac{2n+3}{n+2}xR_{n-1} - \frac{2n+2}{n+2}T_n - \frac{n+1}{n+2}(x^2 + y^2 + z^2)R_{n-2}, \tag{17}$$

with $R_0 = -1$ and $R_1 = -3x$. And the coefficients $c_n(\mu, \beta)$ are given by,

$$c_n(\mu, \beta) = \begin{cases} \frac{1}{\xi_i^3} \left((\pm 1)^n \mu + (-1)^n \frac{(1-\mu)(1-\beta)\xi_i^{n+1}}{(1 \mp \xi_i)^{n+1}} \right), & \text{for } SL_i, i = 1, 2 \\ \frac{(-1)^n}{\xi_3^3} \left((1-\mu)(1-\beta) + \frac{\mu\xi_3^{n+1}}{(1+\xi_3)^{n+1}} \right), & \text{for } SL_3, \end{cases} \tag{18}$$

where the upper sign of the first equation is for SL_1 and the lower sign for SL_2 .

Notice that the change of variables (14) is not canonical, i.e. it does not preserve the Hamiltonian form. But if we apply this change to the equations of motion and introduce the momenta $p_x = \dot{x} - y$, $p_y = \dot{y} + x$ and $p_z = \dot{z}$, the system can also be written in a Hamiltonian form. The expanded Hamiltonian around SL_i is,

$$H_{SL_i} = \frac{1}{2}(p_x^2 + p_y^2 + p_z^2) + yp_x - xp_y - \sum_{n \geq 2} c_n(\mu, \beta)T_n, \tag{19}$$

with c_n and $T_n(x, y, z)$ are as above.

To start the graph transform procedure we need to have the linear part of the system in diagonal form. We take the linear change,

$$(x, y, z, \dot{x}, \dot{y}, \dot{z})^T = C(x_1, x_2, x_3, x_4, y_1, y_2)^T, \tag{20}$$

where C is a matrix that has the eigenvalues of the linear system as columns. This change

takes equation (15) to:

$$\begin{pmatrix} \dot{x}_1 \\ \dot{x}_2 \\ \dot{x}_3 \\ \dot{x}_4 \\ \dot{y}_1 \\ \dot{y}_2 \end{pmatrix} = \left(\begin{array}{cccc|cc} i\omega_1 & 0 & 0 & 0 & \lambda & 0 \\ 0 & -i\omega_1 & 0 & 0 & 0 & -\lambda \\ 0 & 0 & i\omega_2 & 0 & & \\ 0 & 0 & 0 & -i\omega_2 & & \\ \hline & & & & & \end{array} \right) + \begin{pmatrix} f_1(\bar{x}, \bar{y}) \\ f_2(\bar{x}, \bar{y}) \\ f_3(\bar{x}, \bar{y}) \\ f_4(\bar{x}, \bar{y}) \\ g_1(\bar{x}, \bar{y}) \\ g_2(\bar{x}, \bar{y}) \end{pmatrix}. \quad (21)$$

Here $\bar{x} = (x_1, x_2, x_3, x_4)$ are coordinates that have the elliptic character and $\bar{y} = (y_1, y_2)$ the ones with the hyperbolic character, and

$$\begin{pmatrix} f_1(\bar{x}, \bar{y}) \\ f_2(\bar{x}, \bar{y}) \\ f_3(\bar{x}, \bar{y}) \\ f_4(\bar{x}, \bar{y}) \\ g_1(\bar{x}, \bar{y}) \\ g_2(\bar{x}, \bar{y}) \end{pmatrix} = C^{-1} \begin{pmatrix} 0 \\ 0 \\ 0 \\ \sum_{n \geq 2} (n+1)c_{n+1}T_n(\bar{x}, \bar{y}) \\ y(\bar{x}, \bar{y}) \sum_{n \geq 2} c_{n+1}R_{n-1}(\bar{x}, \bar{y}) \\ z(\bar{x}, \bar{y}) \sum_{n \geq 2} c_{n+1}R_{n-1}(\bar{x}, \bar{y}) \end{pmatrix}, \quad (22)$$

are the non - linear terms of the system expressed in the canonical set of coordinates. Notice that the homogeneous polynomials $T_n(\bar{x}, \bar{y})$ and $R_n(\bar{x}, \bar{y})$ are also found in a recurrent way by composing the recurrences (16) and (17) with the linear change (20).

3.2 Results

3.2.1 For the Graph Transform Method

We have applied the graph transform algorithm to the collinear points SL_1 and SL_2 for $\beta = 0.051689$. We have computed the reduction to the centre manifold, finding $y = \hat{v}(x)$ up to degree $N = 32$. Using an Intel Xeon CPU at 3.40GHz this takes around 14min of CPU time. We must mention that although the system has symmetries we have not taken them into account to reduce the computational cost of this algorithm.

In Tables 1 and 2 we can find the first terms of the expansion around SL_1 and SL_2 respectively. To have an approximate idea of the radius of convergence of these series, we have computed numerically the values,

$$r_{i,n} = \sqrt[n]{\|v_n^i\|_1}, \quad \text{where} \quad \|v_n^i\|_1 = \sum_{|k|=n} |v_k^i|, \quad \text{for } 3 \leq n \leq N, \quad i = 1, 2, \quad (23)$$

where the $v_k = (v_k^1, v_k^2)$ are the coefficients of the monomials x^k . Due to the symmetries of the

system, one can see that $r_{1,n} = r_{2,n}$. In Figure 3 we can see how these values behave for SL_1 (left) and SL_2 (right). They give an idea of the radius of convergence of the series, we can appreciate that the divergence is very mild. We can see that the radius of convergence around SL_2 is larger than for SL_1 , but in both cases, for $N = 32$, we have a big neighbourhood where $\hat{v}(x)$ gives a good approximation of the centre manifold.

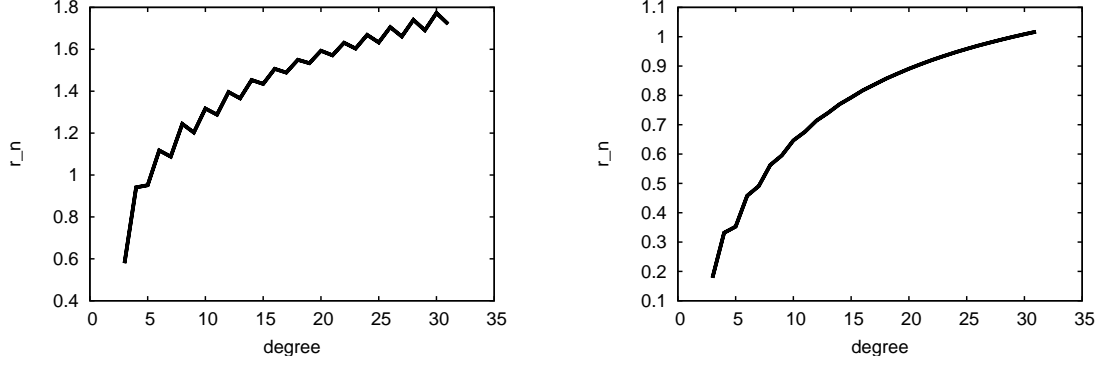


Figure 3: Graph transform method. In both pictures, the horizontal axis corresponds to the value of n and the vertical axis the values of $r_{1,n}$. From left to right: SL_1 and SL_2 .

| k_1 | k_2 | k_3 | k_4 | v_1 | v_2 |
|-------|-------|-------|-------|-------------------------|-------------------------|
| 2 | 0 | 0 | 0 | 3.5503156002936700e-02 | -3.5503156002936700e-02 |
| 1 | 1 | 0 | 0 | 1.7843417171635231e-02 | 1.7843417171635231e-02 |
| 0 | 2 | 0 | 0 | -2.6573244051375060e-03 | 2.6573244051375060e-03 |
| 0 | 0 | 2 | 0 | 3.8147437616048621e-02 | -3.8147437616048621e-02 |
| 0 | 0 | 1 | 1 | 2.3407017142791586e-02 | 2.3407017142791586e-02 |
| 0 | 0 | 0 | 2 | 2.8553303366754226e-02 | -2.8553303366754226e-02 |
| 3 | 0 | 0 | 0 | 5.4460164162132164e-03 | 5.4460164162132164e-03 |
| 2 | 1 | 0 | 0 | 5.6846959570042113e-02 | -5.6846959570042113e-02 |
| 1 | 2 | 0 | 0 | 2.0967349558704437e-02 | 2.0967349558704437e-02 |
| 0 | 3 | 0 | 0 | 1.0668187765301932e-02 | -1.0668187765301932e-02 |
| 1 | 0 | 2 | 0 | 7.8717031446172217e-03 | 7.8717031446172217e-03 |
| 0 | 1 | 2 | 0 | 4.3276556790009330e-02 | -4.3276556790009330e-02 |
| 1 | 0 | 1 | 1 | 2.2839087896562357e-02 | -2.2839087896562357e-02 |
| 0 | 1 | 1 | 1 | 5.0473597730196974e-02 | 5.0473597730196974e-02 |
| 1 | 0 | 0 | 2 | -2.0822825309227966e-02 | -2.0822825309227966e-02 |
| 0 | 1 | 0 | 2 | 2.0724575602143303e-02 | -2.0724575602143303e-02 |

Table 1: Graph transform method. Coefficients of the series $y = v(x)$ truncated at degree 3 at SL_1 for $\beta = 0.051689$. The exponents (k_1, k_2, k_3, k_4) refer to the variables (x_1, x_2, x_3, x_4) .

3.2.2 For the Lies Series Method

We have adapted the public domain library in [6] to the RTBPS for a perpendicular Solar Sail. As before, we have computed the expansion of the Hamiltonian restricted to the centre

| k_1 | k_2 | k_3 | k_4 | v_1 | v_2 |
|-------|-------|-------|-------|-------------------------|-------------------------|
| 2 | 0 | 0 | 0 | -1.7506883374566809e-02 | 1.7506883374566816e-02 |
| 1 | 1 | 0 | 0 | -1.2343035113662425e-02 | -1.2343035113662429e-02 |
| 0 | 2 | 0 | 0 | -7.2504422613208584e-03 | 7.2504422613208618e-03 |
| 0 | 0 | 2 | 0 | -7.3684573354681898e-03 | 7.3684573354681907e-03 |
| 0 | 0 | 1 | 1 | -5.2066907353733706e-03 | -5.2066907353733715e-03 |
| 0 | 0 | 0 | 2 | -3.8210740887108276e-03 | 3.8210740887108284e-03 |
| 3 | 0 | 0 | 0 | 9.3579427535247063e-04 | 9.3579427535247226e-04 |
| 2 | 1 | 0 | 0 | 7.3357172296303003e-03 | -7.3357172296303046e-03 |
| 1 | 2 | 0 | 0 | 3.9348506952868612e-03 | 3.9348506952868630e-03 |
| 0 | 3 | 0 | 0 | -9.2663856231447583e-04 | 9.2663856231447615e-04 |
| 1 | 0 | 2 | 0 | 3.9174272108506583e-04 | 3.9174272108506638e-04 |
| 0 | 1 | 2 | 0 | 1.9200159376202099e-03 | -1.9200159376202108e-03 |
| 1 | 0 | 1 | 1 | 1.1589233890467723e-03 | -1.1589233890467725e-03 |
| 0 | 1 | 1 | 1 | 1.8215774769214797e-03 | 1.8215774769214806e-03 |
| 1 | 0 | 0 | 2 | -1.0501465169187070e-04 | -1.0501465169187056e-04 |
| 0 | 1 | 0 | 2 | -4.7627117583130449e-04 | 4.7627117583130439e-04 |

Table 2: Graph transform method. Coefficients of the series $y = v(x)$ truncated at degree 3 at SL_2 for $\beta = 0.051689$. The exponents (k_1, k_2, k_3, k_4) refer to the variables (x_1, x_2, x_3, x_4) .

manifold up to degree $N = 32$ at the collinear equilibrium points SL_1 and SL_2 respectively, for $\beta = 0.051689$. Using an Intel Xeon CPU at 3.40GHz this takes around 33min of CPU time. We must mention that this software does take into account the symmetries of the problem to reduce the computational effort. It can be seen [7] that the computing time is roughly doubled if the symmetries are not taken into account.

In Tables 3 and 4 we can find the first terms of these expansions. To have an idea of the radius of convergence of the series we have computed numerically the values,

$$r_n = \sqrt[n]{\|H_n\|_1}, \quad \text{where} \quad \|H_n\|_1 = \sum_{|k|=n} |h_k|, \quad \text{for } 3 \leq n \leq N, \quad (24)$$

where the h_k are the coefficients of the monomials x^k . In Figure 4 we can see these values for SL_1 (left) and SL_2 (right). They give an idea of the radius of convergence of the series, we can appreciate that the divergence is very mild. Notice that for SL_2 the radius of convergence is larger than for SL_1 , but in both cases for $N = 32$ we have a big neighbourhood where the modified \widehat{H} gives a good approximation of the dynamics.

3.3 Tests and Comparisons

First, we will discuss some checks that we have done on our programs. Second we will compare the efficiency of both algorithms in terms of computational time.

Let us take an initial condition u_0 on the centre manifold and let u_1 be the result of integrating u_0 on the centre manifold up to time t_1 . We send these two points through the

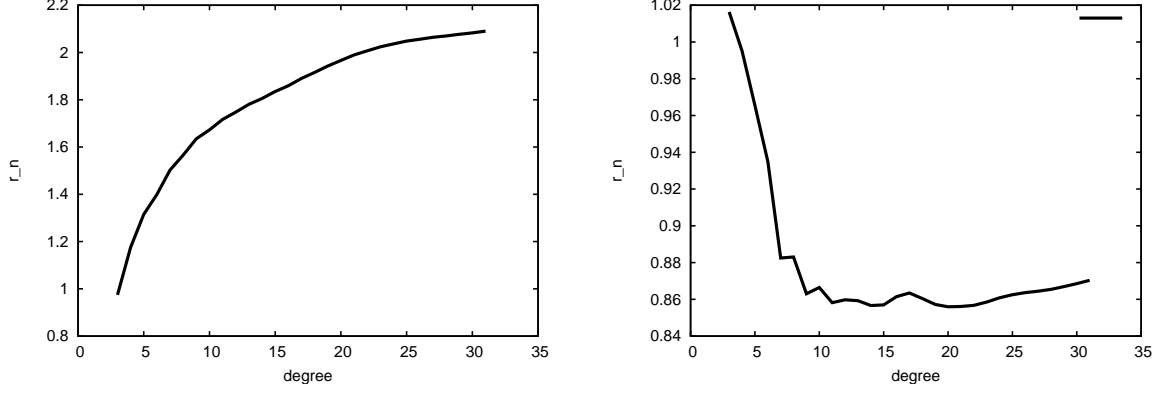


Figure 4: *Lie series method*. In both pictures, the horizontal axis corresponds to the value of n and the vertical axis the values of r_n . From left to right: SL_1 and SL_2 .

| k_1 | k_2 | k_3 | k_4 | h_k | k_1 | k_2 | k_3 | k_4 | h_k |
|-------|-------|-------|-------|-------------------------|-------|-------|-------|-------|-------------------------|
| 2 | 0 | 0 | 0 | 6.2265667517669143e-01 | 0 | 0 | 2 | 2 | 2.5079559432629472e-02 |
| 0 | 2 | 0 | 0 | 6.2265667517669143e-01 | 4 | 1 | 0 | 0 | -9.5850794092866431e-01 |
| 0 | 0 | 2 | 0 | 5.8841603727373581e-01 | 2 | 3 | 0 | 0 | 8.9664076808524873e-01 |
| 0 | 0 | 0 | 2 | 5.8841603727373581e-01 | 0 | 5 | 0 | 0 | -2.4981368648887291e-02 |
| 2 | 1 | 0 | 0 | 5.6396639629808476e-01 | 2 | 1 | 2 | 0 | -7.9713058687831795e-01 |
| 0 | 3 | 0 | 0 | -8.2384619895258443e-02 | 0 | 3 | 2 | 0 | 2.9651411265486743e-01 |
| 0 | 1 | 2 | 0 | 2.7889905508879165e-01 | 3 | 0 | 1 | 1 | -1.4808514924214936e-01 |
| 4 | 0 | 0 | 0 | -2.7269463441025565e-01 | 1 | 2 | 1 | 1 | 1.9692859885303951e-01 |
| 2 | 2 | 0 | 0 | 7.5895544668314852e-01 | 2 | 1 | 0 | 2 | 2.0424400532712889e-01 |
| 0 | 4 | 0 | 0 | -4.8826949550717223e-02 | 0 | 3 | 0 | 2 | -3.5255336989995716e-02 |
| 2 | 0 | 2 | 0 | -2.7377958223456894e-01 | 0 | 1 | 4 | 0 | -1.5996695825115495e-01 |
| 0 | 2 | 2 | 0 | 3.2741624078653092e-01 | 1 | 0 | 3 | 1 | -7.4332299532813700e-02 |
| 1 | 1 | 1 | 1 | 5.7170659054552292e-02 | 0 | 1 | 2 | 2 | 1.1973274094713404e-01 |
| 2 | 0 | 0 | 2 | 5.0713792305465924e-02 | 1 | 0 | 1 | 3 | 1.3709284563953436e-02 |
| 0 | 2 | 0 | 2 | -2.2224922601547636e-02 | 0 | 1 | 0 | 4 | -8.0914094767427763e-03 |
| 0 | 0 | 4 | 0 | -6.8702044013507921e-02 | | | | | |

Table 3: *Lie series method*. Coefficients up to degree 5, of the Hamiltonian restricted to the centre manifold at SL_1 for $\beta = 0.051689$. The exponents (k_1, k_2, k_3, k_4) refer to the variables (q_2, p_2, q_3, p_3) .

change of variables to the complete system. Let v_0 and v_1 be these points. Now we take v_0 and integrate it up to time t_1 on the full system, let us call this point w_1 .

Ideally, if the centre manifold, the change of variables and the numerical integrations were all exact, the difference between w_1 and v_1 would be zero. As we know, this will not be true due to the several sources of errors.

Let us define $h_0 = \|u_0\|$ and we compute $\|v_1 - w_1\|_2$. This quantity is affected by the truncation order of the reduction to the centre manifold process, the truncation error of the integrating method and the roundoff error due to the operations. We can choose the integration time t_1 and the distance to the origin h_0 , in a way that $\|v_1 - w_1\|_2$ is mainly affected by the truncation order of the centre manifold. Then this quantity should behave as $\xi h_0^{(N+1)}$ where N is the last order that we have taken into account in the centre manifold.

| k_1 | k_2 | k_3 | k_4 | h_k | k_1 | k_2 | k_3 | k_4 | h_k |
|-------|-------|-------|-------|-------------------------|-------|-------|-------|-------|-------------------------|
| 2 | 0 | 0 | 0 | 1.7322989883542399e+00 | 0 | 0 | 2 | 2 | 1.6866624170049516e-01 |
| 0 | 2 | 0 | 0 | 1.7322989883542399e+00 | 4 | 1 | 0 | 0 | 6.0646742774657904e-02 |
| 0 | 0 | 2 | 0 | 1.7090415995033998e+00 | 2 | 3 | 0 | 0 | -1.4911538654097725e-01 |
| 0 | 0 | 0 | 2 | 1.7090415995033998e+00 | 0 | 5 | 0 | 0 | 1.3665081880113589e-02 |
| 2 | 1 | 0 | 0 | -5.3481429234647238e-01 | 2 | 1 | 2 | 0 | 5.5825772462267019e-02 |
| 0 | 3 | 0 | 0 | 1.2941667603118245e-02 | 0 | 3 | 2 | 0 | -6.9102572140442006e-02 |
| 0 | 1 | 2 | 0 | -5.0214927846709145e-01 | 3 | 0 | 1 | 1 | 5.3708550049071303e-02 |
| 4 | 0 | 0 | 0 | -2.4049000215462642e-02 | 1 | 2 | 1 | 1 | -1.1553805534006134e-01 |
| 2 | 2 | 0 | 0 | 2.6749334664134067e-01 | 2 | 1 | 0 | 2 | -9.5244592428503097e-02 |
| 0 | 4 | 0 | 0 | -1.2415552501629217e-02 | 0 | 3 | 0 | 2 | 2.8431961390884643e-02 |
| 2 | 0 | 2 | 0 | -4.3825787410913676e-02 | 0 | 1 | 4 | 0 | -8.8476587697261728e-04 |
| 0 | 2 | 2 | 0 | 2.2438948116603341e-01 | 1 | 0 | 3 | 1 | 5.0249628386339631e-02 |
| 1 | 1 | 1 | 1 | 2.6832801596053099e-02 | 0 | 1 | 2 | 2 | -1.0765378366189296e-01 |
| 2 | 0 | 0 | 2 | 1.7963804901434496e-01 | 1 | 0 | 1 | 3 | -2.4034222457073172e-02 |
| 0 | 2 | 0 | 2 | -1.3040877660634168e-02 | 0 | 1 | 0 | 4 | 1.4721820971207975e-02 |
| 0 | 0 | 4 | 0 | -1.9948009163984572e-02 | | | | | |

Table 4: *Lie series method. Coefficients up to degree 5, of the Hamiltonian restricted to the centre manifold at SL_2 for $\beta = 0.051689$. The exponents (k_1, k_2, k_3, k_4) refer to the variables (q_2, p_2, q_3, p_3) .*

We can take two different initial conditions, $u_0^{(1)}$ and $u_0^{(2)}$, and estimate N by,

$$N + 1 \approx \frac{\log\left(\frac{er_1}{er_2}\right)}{\log\left(\frac{h_0^{(1)}}{h_0^{(2)}}\right)}, \quad (25)$$

where $er_i = \|v_1^{(i)} - w_1^{(i)}\|$ and $h^{(i)} = \|u_0^{(i)}\|$ for $i = 1, 2$.

We have taken the centre manifold around SL_1 and SL_2 computed using the graph transform method and used it to integrate on the centre manifold. We have taken an initial condition on the centre manifold $u_0 = (h_0, h_0, h_0, h_0)$ and computed v_1 and w_1 for $t_1 = 0.01$. In Table 5 we can see the local error of the numerical integration truncating the series at degree 8. It illustrates the good approximation of the dynamics on the centre manifold that this gives. In Table 6 we see the estimates of the truncation error.

We have done the same taking the transformed Hamiltonian around SL_1 and SL_2 computed using the Lie Series method. In Table 7 we can see the local error of the numerical integration taking the truncated Hamiltonian up to degree 8 and in Table 8 we see the estimates of the truncation error using equation (25). Notice that we truncate the Hamiltonian up to degree 8, hence the estimation of the truncation error will be 8 as the set of equations that we are integrating are taken up to degree 7.

Notice that Tables 5 and 7 give us an idea of how good is the approximation of the motion on the approximation of the centre manifold truncated at degree 8. The same computations can be done taking the centre manifolds approximation truncated at a given degree N . The higher the degree is, the better approximation will be. However, due to the divergence in

| h_0 | $\ v_1 - w_1\ $ |
|-------|------------------------|
| 0.02 | 1.2139221824443741e-17 |
| 0.04 | 2.3643249923959272e-15 |
| 0.08 | 1.2618898774811476e-12 |
| 0.16 | 6.9534006796827247e-10 |
| 0.32 | 3.9879163406944996e-07 |

| h_0 | $\ v_1 - w_1\ $ |
|-------|------------------------|
| 0.02 | 2.5146775308808859e-17 |
| 0.04 | 1.8662949690767610e-16 |
| 0.08 | 9.6561350589145246e-14 |
| 0.16 | 4.8655084457371298e-11 |
| 0.32 | 2.4673928463137270e-08 |

Table 5: For the graph transform method: difference between the numerical integration on the centre manifold and on the RTBPS taking initial conditions at a distance h_0 from the origin. Taking the series $y = v(x)$ truncated at degree 8 at SL_1 (left) and at SL_2 (right) for $\beta = 0.051689$.

| $h_0^{(1)}$ | $h_0^{(2)}$ | $N + 1$ |
|-------------|-------------|---------|
| 0.02 | 0.04 | 4.44043 |
| 0.04 | 0.08 | 9.02389 |
| 0.08 | 0.16 | 9.10595 |
| 0.16 | 0.32 | 9.16370 |

| $h_0^{(1)}$ | $h_0^{(2)}$ | $N + 1$ |
|-------------|-------------|----------|
| 0.02 | 0.04 | 2.629343 |
| 0.04 | 0.08 | 8.764844 |
| 0.08 | 0.16 | 8.976466 |
| 0.16 | 0.32 | 8.986181 |

Table 6: For the graph transform method: estimations of the truncation order for $\widehat{v}(x)$. For $\beta = 0.051689$ at SL_1 (left) and at SL_2 (right).

the centre manifold, the distance in which we have a the good approximation for very large N can be small.

As we have already mentioned, the graph transform method is a more general approach, as it does not use any assumption on the set of equations, while the Lie series method can only be applied to Hamiltonian systems. Now we will compare the efficiency in terms of computational time of both methods.

We have computed the centre manifold up to degree 8, 16, 24, and 32 using the two approaches. All the computations have been done on the same computer, with an Intel(R) Core(TM)2 Quad CPU at 2.83GHz. In Table 9 we have the CPU time needed to compute each of them. Notice that, despite not taking into account the symmetries of the problem, the graph transform algorithm is more efficient, in terms of computational time, than the Lie series approach.

With the Lie series approach, we take the Hamiltonian function, expand it around the fixed point, and by means of canonical transformation decouple up to high order the hyperbolic directions from the elliptic ones. Hence, during the whole process we deal with homogeneous polynomials with 6 variables and at the end of the process we set two of the variables to zero, to end on a 4D phase space.

On the other hand, with the graph transform method, we compute the power expansion of the local centre manifold ($y = v(x)$). We see that $v(x)$ must satisfy an invariant equation, that we solve equalising degree by degree. Now, during the whole process we deal with homogeneous polynomials with 4 variables, which coincides with the dimension of the final phase space.

| h_0 | $\ v_1 - w_1\ $ |
|-------|------------------------|
| 0.02 | 3.6920450235560199e-15 |
| 0.04 | 9.4549612587473395e-13 |
| 0.08 | 2.4173024466492310e-10 |
| 0.16 | 6.4090169252390676e-08 |
| 0.32 | 2.1474173035560701e-05 |

| h_0 | $\ v_1 - w_1\ $ |
|-------|------------------------|
| 0.02 | 3.9057253333709475e-15 |
| 0.04 | 1.8756915513177915e-14 |
| 0.08 | 9.7024896946065764e-13 |
| 0.16 | 2.2668434557013075e-10 |
| 0.32 | 5.4714331083417134e-08 |

Table 7: For the Lie series method: difference between the numerical integration on the centre manifold and on the RTBPS taking initial conditions at a distance h_0 from the origin. Taking the series H_N truncated at degree 8 at SL_1 (left) and at SL_2 (right) for $\beta = 0.051689$.

| $h_0^{(1)}$ | $h_0^{(2)}$ | N |
|-------------|-------------|-------|
| 0.02 | 0.04 | 8.001 |
| 0.04 | 0.08 | 7.998 |
| 0.08 | 0.16 | 8.051 |
| 0.16 | 0.32 | 8.388 |

| $h_0^{(1)}$ | $h_0^{(2)}$ | N |
|-------------|-------------|-------|
| 0.02 | 0.04 | 2.263 |
| 0.04 | 0.08 | 5.692 |
| 0.08 | 0.16 | 7.868 |
| 0.16 | 0.32 | 7.915 |

Table 8: For the Lie series method: estimations of the truncation order for the reduction to the centre manifold for H_8 . For $\beta = 0.051689$ at SL_1 (left) and at SL_2 (right).

| N | Lie Series | Graph Transform |
|----|-------------|-----------------|
| 8 | 0m 0.085s | 0m 0.057s |
| 16 | 0m 3.876s | 0m 2.943s |
| 24 | 2m 10.251s | 1m 13.965s |
| 32 | 33m 22.000s | 14m 35.475s |

Table 9: Computational time for Lie Series vs the Graph Transform method to compute the reduction to the centre manifold up to degree N .

Under general conditions, the cost of operating with polynomials of 4 variables is much less than the cost of operating with polynomials of 6 variables.

Although it is less efficient, the Lie series approach is convenient when we have a Hamiltonian system, as we end up with a very good approximation of the Hamilton equation on the centre manifold, and we preserve most of the interesting properties of the system. The Hamilton equation is very useful to study the phase space, we use this first integral to reduce the phase space dimension.

3.4 Dynamics on the Centre Manifold

Here we use the reduction to the centre manifold to understand the dynamics around the equilibrium points SL_1 and SL_2 . The results that we present are done considering the reduction done by the graph transform method, although the same can be done with the approximation of the centre manifold obtained with the Lie series method.

We recall that once we have found $y = \hat{v}(x)$, a high order approximation of the graph

of the centre manifold, we take $\dot{x} = Ax + f(x, \widehat{v}(x))$ to integrate the flow on the centre manifold. Now we are in a four dimensional phase space (x_1, x_2, x_3, x_4) where plots are hard to visualise. We will take suitable sections to reduce the phase space dimension and make this easier.

We have taken a Poincaré section $x_3 = 0$ and fixed several energy levels h to determine x_4 . Notice that taking $x_3 = 0$ is like taking $Z = 0$, and x_4 is related to \dot{Z} . Hence, the subspace $\{x_1, x_2\}$ is a linear transformation of a subspace in the $\{x, y, p_x, p_y\}$ - space. We will take different energy levels h , for each h we have taken different initial conditions and computed 500 iterates on the Poincaré section. In Figures 5 and 6 we can see the results around SL_1 and SL_2 respectively.

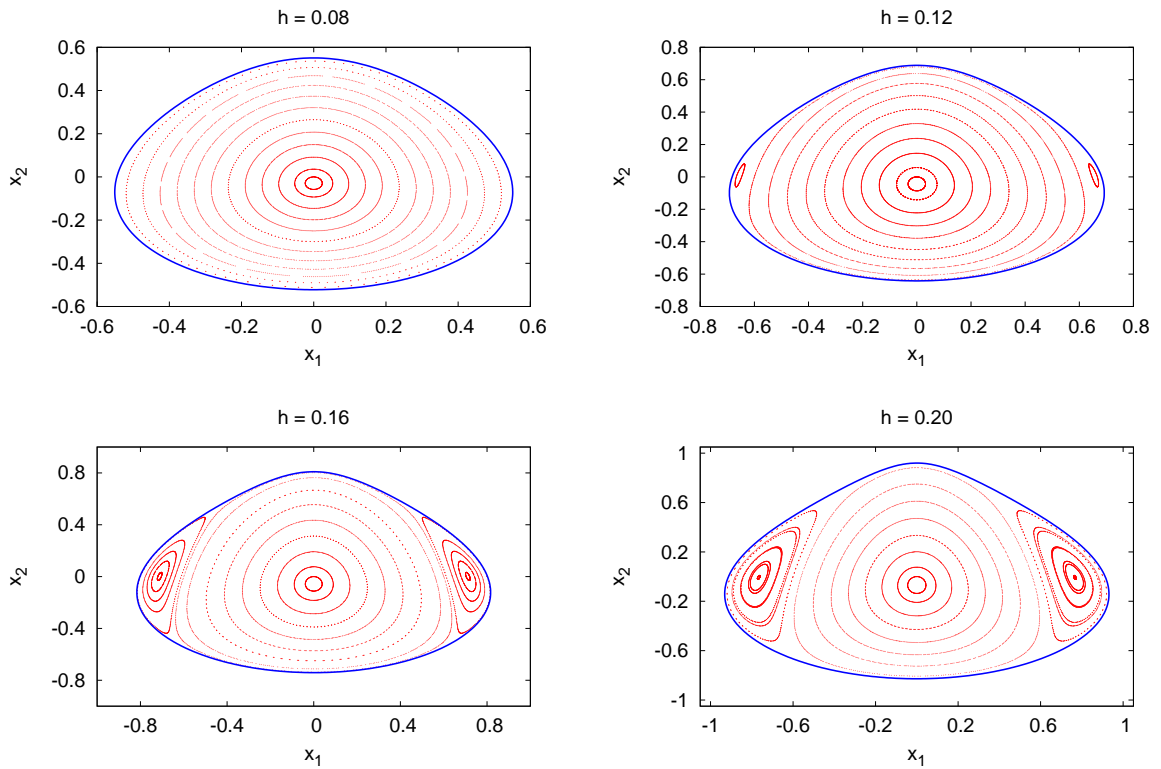


Figure 5: Poincaré sections around SL_1 for $\beta = 0.051689$, for different energy levels. From left to right, top to bottom: $h = 0.08$, $h = 0.12$, $h = 0.16$, $h = 0.2$. The continuous line is the planar Lyapunov periodic orbit for each that energy level.

We observe that the motion around both equilibrium points is qualitatively the same. The two frequencies (ω_1 and ω_2) that define the central motion give rise to two families of periodic orbits, the planar and vertical Lyapunov orbits, parametrised by the energy h . The planar Lyapunov orbit is totally contained in the $x_3 = 0$ plane, it is seen as a continuous line in Figures 5 and 6. The vertical Lyapunov orbit crosses transversally the Poincaré section and is seen as a fixed point close to the origin. The interaction of the two frequencies gives

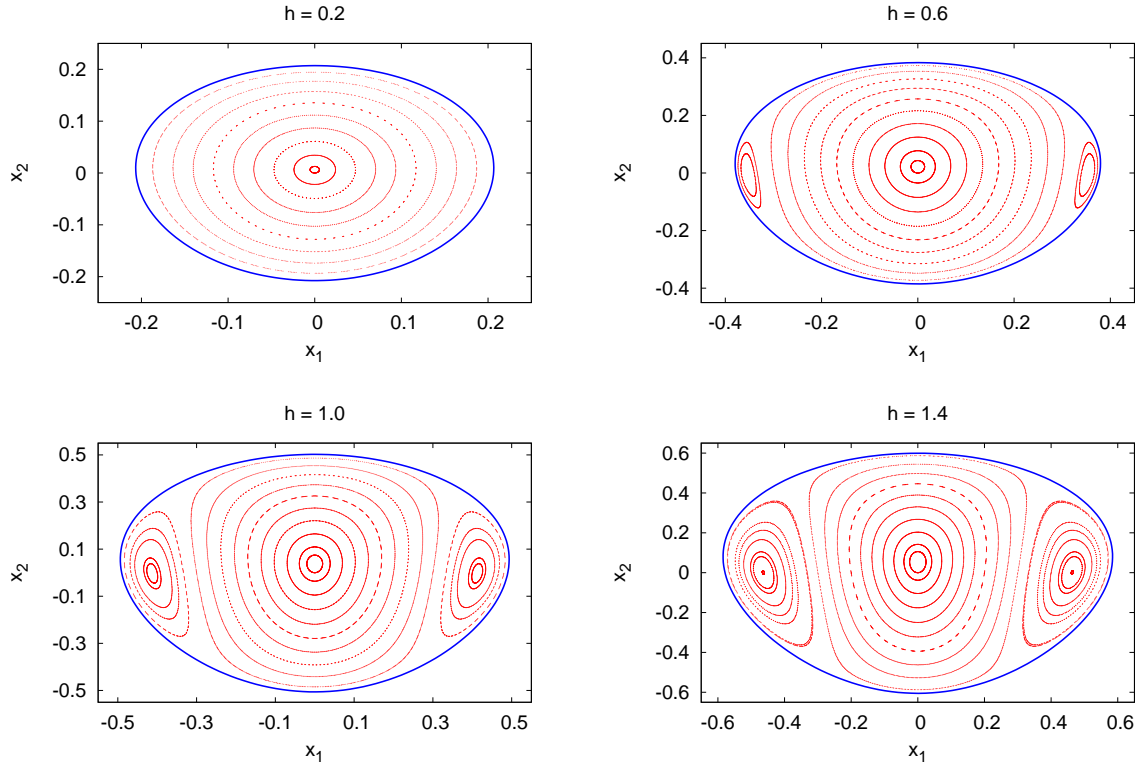


Figure 6: *Poincaré sections around SL_2 for $\beta = 0.051689$, for different energy levels. From left to right, top to bottom: $h = 0.2$, $h = 0.6$, $h = 1.0$, $h = 1.4$. The continuous line is the planar Lyapunov periodic orbit for each that energy level.*

rise to a family of invariant tori around the fixed point, sometimes called Lissajous orbits.

As we can see in Figures 5 and 6, for each energy level the quasi - periodic motion on the Poincaré section is bounded by the planar Lyapunov orbit. As the energy level increases, the planar Lyapunov orbit changes its stability and gives rise to two Halo orbits, that are transversal to this section and are the two symmetric fixed points w.r.t $x_1 = 0$ that appear.

The main quantitative difference between the behaviour around SL_1 and SL_2 is when the Halo orbits appear. We can see that around SL_1 the bifurcation takes place between $h_1 = 0.1$ and $h_2 = 0.12$, while for SL_2 this happens $h_1 = 0.4$ and $h_2 = 0.6$.

4 Conclusions

We are interested in understanding the dynamics close to unstable equilibrium point. We have used the *graph transform method* to compute reduction to the centre manifold. The idea is to compute, formally, the power expansion of the graph of the local centre manifold ($y = v(x)$). We have seen that $v(x)$ must satisfy an invariant equation, that we solve by expanding all of the terms of this equation and equalising degree by degree up to a sufficiently

high order. This can be done in an iterative way by solving at each step a linear system.

In Section 2.1 we have described the main details of this algorithm. We have also shown how to use recurrent expressions for the expansion of the non - linear terms to reduce the computational effort of this algorithm.

In Section 3.3 we have compared this method with a more classical approach to this problem. If the system is Hamiltonian one can also use a Lie series method, taking advantage of the Hamiltonian structure of the system. We have taken the public domain software in [6], that deals with the reduction to the centre manifold around a collinear equilibrium point for the RTBP, and adapted it to our model.

We have seen that the graph transform method, using recurrent expressions for the non - linear terms, is more efficient in terms of computational time than the Lie series method. Moreover, this method gives a more general approach to the problem. It has been used to study the non - linear dynamics around the equilibrium points when the sail is not orientated perpendicular to the Sun - line [2].

Finally, we have used the reduction to the centre manifold to describe the motion of a Solar sail in the RTBPS around the collinear points SL_1 and SL_2 . We have computed the reduction to the centre manifold up to degree 32 around these two points. To visualise the phase space behaviour, we have fixed different energy levels and set the Poincaré section $Z = 0$. Notice that this is the only point in the whole process that we take advantage of the Hamiltonian structure of the system.

We have seen that the qualitative behaviour around the different equilibrium points is the same. In both cases we have planar and vertical family of periodic orbits that are given by the two frequencies defining the centre motion. For each energy level we also find families of invariant tori around the equilibrium point, that are bounded on the Poincaré section by the planar Lyapunov orbit. As the energy level increases, the planar Lyapunov family changes its stability and gives rise to two Halo orbits. We must note that the system behaves very similar to the classical RTBP around L_1 and L_2 .

Acknowledgements

This work has been supported by the MEC grant MTM2006-11265 and the CIRIT grant 2005SGR01028.

References

- [1] J. Carr. *Applications of Centre Manifold Theory*, volume 35 of *Applied Mathematical Series*. Springer-Verlag, New York, 1981.

- [2] A. Farrés and À. Jorba. Periodic and quasi-periodic motions of a solar sail around the family SL_1 on the Sun - Earth system. In progress.
- [3] R. L. Forward. Statite: A spacecraft that does not orbit. *Journal of Spacecraft*, 28(5):606–611, 1990.
- [4] G. Gómez, À. Jorba, J. Masdemont, and C. Simó. *Dynamics and Mission Design Near Libration Points - Volume III: Advanced Methods for Collinear Points.*, volume 4 of *World Scientific Monograph Series in Mathematics*. World Scientific, 2001.
- [5] A. Haro. Automatic differentiation tools in computational dynamical systems. Preprint, 2008.
- [6] À. Jorba. <http://www.maia.ub.es/~angel/soft.html>.
- [7] À. Jorba. A methodology for the numerical computation of normal forms, centre manifolds and first integrals of hamiltonian systems. *Experimental Mathematics* 8, pages 155–195, 1999.
- [8] À. Jorba and J. Masdemont. Dynamics in the centre manifold of the collinear points of the restricted three body problem. *Physica D* 132, pages 189–213, 1999.
- [9] D. Knuth. *The art of computer programming. Vol. 2*. Addison-Wesley Publishing Co., Reading, Mass., second edition, 1981. Seminumerical algorithms, Addison-Wesley Series in Computer Science and Information Processing.
- [10] C. McInnes. *Solar Sailing: Technology, Dynamics and Mission Applications*. Springer-Praxis, 1999.
- [11] C. McInnes, A. McDonald, J. Simmons, and E. MacDonald. Solar sail parking in restricted three-body system. *Journal of Guidance, Control and Dynamics*, 17(2):399–406, 1994.
- [12] D. Richardson. A note on a Lagrangian formulation for motion about the collinear points. *Celestial Mechanics*, 22:231–236, 1980.
- [13] P. Roldán. *Analytical and Numerical Tools for the study of Normally Hyperbolic Invariant Manifolds in Hamiltonian Systems and their associated dynamics*. PhD thesis, Universitat Politècnica de Barcelona, 2007.
- [14] J. Sijbrand. Properties of the centre manifold. *Transactions of the American Mathematical Society*, 289(2), June 1985.

- [15] C. Simó. On the analytical and numerical approximation of invariant manifolds. In D. Benest and C. Froeschlé, editors, *Modern methods in celestial mechanics*, pages 285–330. Ed. Frontières, 1990.
- [16] V. Szebehely. *Theory of orbits. The restricted problem of three bodies*. Academic Press, 1967.
- [17] A. Vanderbauwhede. *Centre Manifolds, Normal Forms and Elementary Bifurcations*, chapter 4. Dynamics Reported. A Series in Dynamical Systems and their Applications, Vol. 2. John Wiley & Sons Ltd., 1989.